



**HAL**  
open science

# Fiber/matrix debonding criterions in SiC/Ti composite numerical and experimental analysis

Alain Thionnet, Jacques Renard

► **To cite this version:**

Alain Thionnet, Jacques Renard. Fiber/matrix debonding criterions in SiC/Ti composite numerical and experimental analysis. ICCM 12, Jul 1999, Paris, France. 8 p. hal-01843135

**HAL Id: hal-01843135**

**<https://hal-mines-paristech.archives-ouvertes.fr/hal-01843135>**

Submitted on 18 Jul 2018

**HAL** is a multi-disciplinary open access archive for the deposit and dissemination of scientific research documents, whether they are published or not. The documents may come from teaching and research institutions in France or abroad, or from public or private research centers.

L'archive ouverte pluridisciplinaire **HAL**, est destinée au dépôt et à la diffusion de documents scientifiques de niveau recherche, publiés ou non, émanant des établissements d'enseignement et de recherche français ou étrangers, des laboratoires publics ou privés.

# FIBER/MATRIX DEBONDING CRITERIONS IN SiC/TI COMPOSITE. NUMERICAL AND EXPERIMENTAL ANALYSIS

A. Thionnet<sup>1+2</sup>, J. Renard<sup>1</sup>

<sup>1</sup>*Ecole Nationale Supérieure des Mines de Paris - Centre des Matériaux P. M. Fourt  
BP 87 - 91003 Evry Cedex - France*

<sup>2</sup>*Université de Bourgogne  
BP 47870 - 21078 Dijon Cedex – France*

**KEYWORDS** : metal matrix composite, debonding, modelling

## INTRODUCTION

As SiC/Ti metal matrix composite have good mechanical properties, they have been chosen these last years for aeronautical applications. In order to increase their utilization, it becomes necessary to detect and analyze the propagation of the various types of damages which occur when the composite structure is loaded.

The linear elastic behaviour of these materials is correctly simulated by homogenization models. However, the dissipative phenomenon as well as the induced non-linearities are still badly understood. The properties and the behaviour of these composite materials depend, not only on the intrinsic constituent properties but also on the interface between the fiber and the matrix. This study analyzes the influence of the debonding between the two constituents.

Our approach is carried out both experimentally and numerically. For each of these two investigations, we first analyze the phenomenon at the microscopic scale (where we distinguish the constituents of the heterogeneous material) and then its influence on the mesoscopic scale (where we do not distinguish anymore the constituents of the material now become homogeneous). Experimentally, the use of fine analysis technics (optical microscopy, spectrometry...) enables to observe the debonding phenomenon at its microscopic scale. Then, experiments allow to quantify the influence of the phenomenon at the mesoscopic scale. Numerically, the microscopic phenomenon is analyzed using a finite element calculation with a mesh having the scale of the fiber and the matrix where the debonding is realized by penalties. A homogenization process helps to reach the mesoscopic scale and evaluate the influence of the degradation on the behaviour of the equivalent homogeneous material. Finally, the numerical and the experimental response of a composite sample submitted to a transversal traction loading is compared at the macroscopic scale (the scale of the structure). This approach is realised in the both cases with or without taking into account the curing residual stresses.

The originality of the present study is to show the feasibility to get some mesoscopic quantities [1] from microscopic information and observations. One application is the determination of a mesoscopic debonding criterion built up from its local equivalent.

### DESCRIPTION OF THE MATERIAL

The studied composite material is made by hot compaction (950 °C) of 12 SiC long fibers' layers in a titanium metal matrix. The matrix is a "super- $\alpha$ " titanium alloy. The Silicon carbide fibers, the diameter of which is about 100  $\mu\text{m}$  (Fig. 1), are surrounded by a carbon deposit of approximately 2  $\mu\text{m}$  of thickness (Fig. 2). The fiber / matrix debonding arises from the rupture of this zone (Fig. 3). The microstructure of the composite is approximately periodic with a fiber volume fraction of about 0.32, a carbon deposit of 0.01 and a volume fraction of matrix of about 0.67.

The difference between the coefficients of thermal expansion of the reinforcement and the matrix gives the appearance of a residual stress field. These residual stresses can be damageable for the material, as they affect the bonding between the fiber and the matrix. A solution is to introduce an interphase sufficiently smooth between the fiber and the matrix that absorbs gaps of displacement. This is the reason why the fiber presents on its periphery a protective carbon deposit which play this role.

The proposed study analyzes the rupture of this interphase leading to the debonding between the fiber and the matrix (Fig. 3).

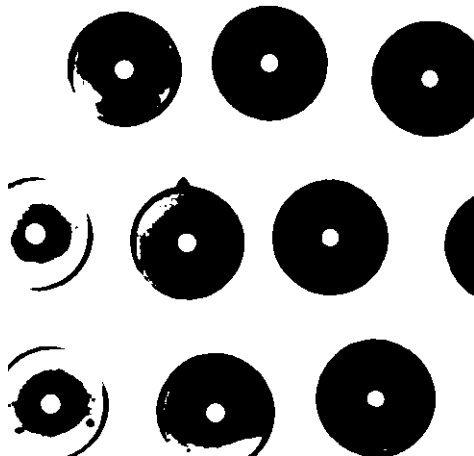


Fig. 1 - Microstructure of the Sic-Ti composite

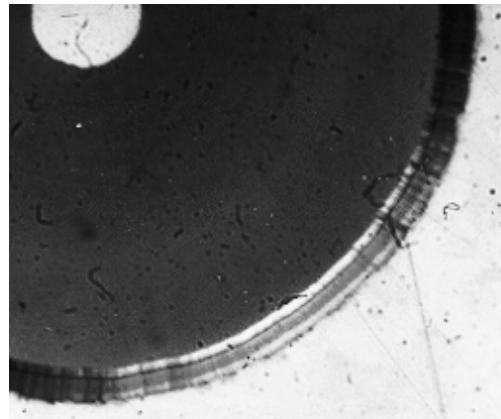


Fig. 2 - Interphase



Fig. 3 - Situation of the debonding phenomenon during a torsion test on a T90 specimen

### EXPERIMENTAL ANALYSIS

At the microscopic level, we observe where and when debonding appears in the representative cell of the material. At the macroscopic level, we record the loading-unloading curve during a test on a sample representative of the elementary volume of the material and the evolution of the number of debondings for different loadings. The used specimen (Fig. 4), called T90, are trilaminar (a SiC-Ti layer between two titanium layers) and such that SiC fibers are located at 90° from the axis of the specimen. (X, Y, Z) is the cartesian frame of the specimen where the X axis is parallel to its length. After polishing the lateral faces and increasing the load, the debondings are observed and counted on a chosen zone of one lateral face (Fig. 4). The same procedure is repeated at each load increase. By this way we follow the surfacial evolution of the debonding.

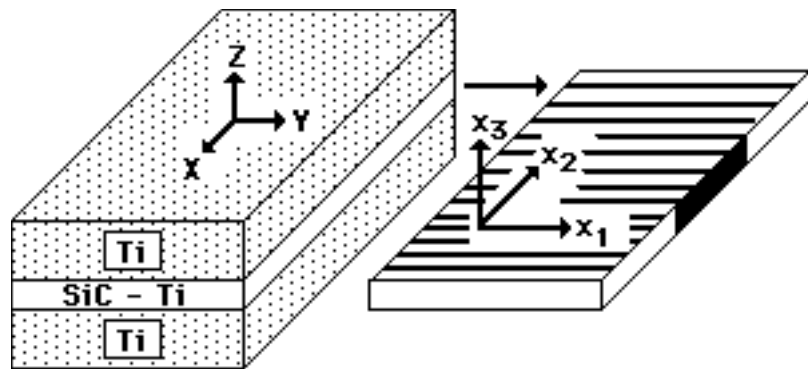


Fig. 4 - Tested specimen (◆ : observed area)

### Choice of the Applied Loading on to the Specimen

To observe the debondings, the specimen was loaded with a torque along the X axis. The used machine allows to apply a linear time-dependant torque. Thus we obtain the evolution of the torque C versus the angle  $\Omega$ . This device has a mobile jaw which avoid some parasite stress during the torsional loading.

The main motivation for the choice of the torsional loading is that the induced state of stress is simple. Indeed, we have simulated the torsion of the T90 specimen by the finite element method using a pseudo-tridimensionnal element. The analysis of the numerical simulation on the lateral side of the specimen shows that only component  $\sigma_{xy}$  and  $\sigma_{xz}$  are non zero. But, if we look more attentively, we observe that in fact only  $\sigma_{xz}$  is not significantly null in the SiC-Ti ply. Thus, if we note  $(x_1, x_2, x_3)$  the local orthotropic frame of the SiC-Ti material where the  $x_1$  axis is parallel to the fibers (Fig. 4), the mesoscopic state of stress in the composite ply of the T90 specimen is the following :

$$\sigma = \begin{pmatrix} 0 & 0 & 0 \\ 0 & 0 & \sigma_{23} \\ 0 & \sigma_{23} & 0 \end{pmatrix}$$

### Superficial Evolution of the Debonding Phenomenon

After loading the T90 specimen we observe the zone of the lateral side. We plot their density  $D_S$  versus the applied torque (Fig. 6) and we record the macroscopic response of the specimen

giving the value of the applied torque according to the angle (Fig. 5). The main conclusion is that the debondings however important seems not affect the global behaviour. Indeed, although we observe a lot of debondings on the specimen faces, nothing proves that they propagate all along the fibers, far in the width of the specimen. To evaluate their penetration, finite element calculations with a homogenization method have been used.

### NUMERICAL ANALYSIS OF THE DEBONDING INFLUENCE ON THE BEHAVIOUR

The homogenization method used suppose periodic properties of the studied composite. Calculations are realized by finite elements method on the representative elementary cell of the material. Calculated characteristics of the homogenized behaviour calculated of our virgin material are relatively in good agreement with the values found experimentally by Robertson [2] on a close material.

Concerning the influence of the debonding on the behaviour of the material, the study is realized using two different ways. First, by simulating really the debonding by splitting the nodes of the mesh between the two primary layers, i.e. on a circle of 1  $\mu\text{m}$  superior to the fiber. This approach induces locally a penetration of the constituents if we do not manage the contact in the case of the shear loadings. Second, we simulate the debonding by weakening a small part of carbon interphase (we have divided by 100 the initial characteristics of the carbon, in a zone of thickness 1.00 mm) situated around the fiber. Results obtained by this method do not give significant difference when compared to the first approach. We suppose a complete debonding what has for consequence to overestimate the stiffness losses.

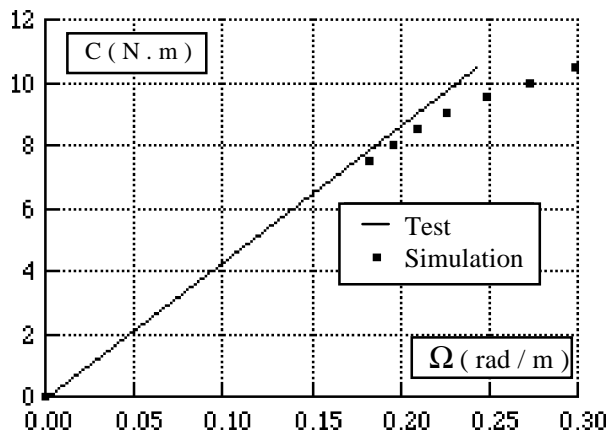


Fig. 5 - Macroscopic response torque/angle for the T90 specimen in torsion

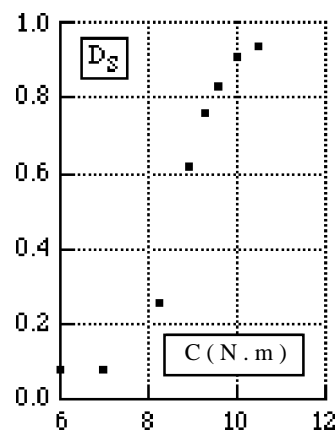


Fig. 6 - Superficial debonding / torque curve

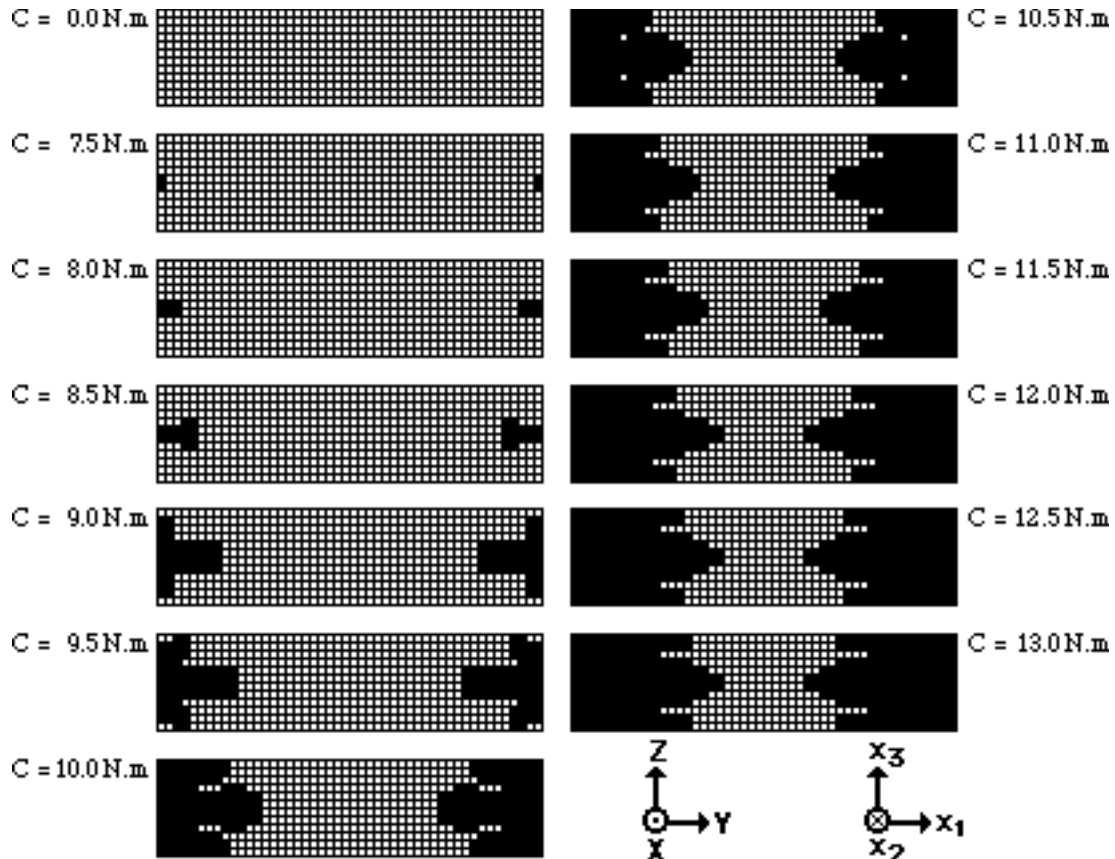


Fig. 7 - Damaged elements cartography in the SiC-Ti layer of the straight section of the T90 specimen in torsion

## NUMERICAL ANALYSIS OF THE VOLUMIC CHARACTER OF THE DEBONDINGS

Experimentally, we get the value of the torque  $C_0$  for which appear the first debondings on the T90 specimen. The finite element calculation gives the critical debonding stress tensor  $\sigma^0$ . To estimate the penetration of these debondings into the material, we realized the simulation of the torsional test by the following steps : we load until the torque  $C_0$  and we look in which elements a debonding critical state of stress has been reached. The damaged behaviour of these elements is calculated during the homogenization step. The torque is then increased, and so on. The cartography of damaged elements indicates the depth of penetration of the debonding (Fig. 7) and we give the torque/angle simulated curve (Fig. 5). Numerically, we observe a decrease of the specimen torsion modulus of approximately 25% while the experimental curve shows no decrease. This can be explained because decreases of material modulus have been overestimated and because the calculation by finite element method is realized with plane strain elements.

## ANALYSIS WITHOUT CONSIDERATION OF THE RESIDUAL STRESSES

### Identification of the Microscopic Debonding Criterion

By applying the mesoscopic state of stress  $\sigma^0$  on the representative cell of the material, the procedure of localization associated with the homogenization gives the microscopic state of stress in all point of this cell. We can therefore access to the normal and tangential strength between the two primary layers, located close the debonding. In besides, a micrography of the

debonding phenomenon (Figs. 8-9) for the torque  $C_0$  allows to understand preceding results and therefore, help to write a microscopic debonding criterion. We call  $\omega$  the area constituted by the fiber and the part of the deposit of carbon that it is always interdependent and  $\partial\omega$  its frontier. By calling  $s$  the microscopic stress tensor, we note  $s \vec{n} = s_T \vec{t} + s_L \vec{x}_1 + s_N \vec{n}$  the stress vector on  $\partial\omega$ , where the unit vectors  $\vec{n}$  and  $\vec{t}$  are respectively oriented with the normal to  $\partial\omega$  et with the tangent at  $\partial\omega$  in the plane of the cross section. A local debonding criterion can be written as :

$$\left( \frac{s_T}{s_T^c} \right)^2 + \left( \frac{s_L}{s_L^c} \right)^2 + \left( \frac{s_N}{s_N^c} \right)^2 = 1$$

where  $s_T^c$  et  $s_L^c$  are the critical tangential values and  $s_N^c$  the critical normal value of debonding. As first approximation, we can estimate  $s_T^c \approx s_L^c$  and here the simulations give :  $s_T^c \approx s_L^c \approx 30$  MPa and  $s_N^c \approx 70$  MPa. However, in the literature, we find  $s_L^c \approx 150$  MPa [3]. Although constituents and the process of elaboration of the composite are not rigorously identical, these values indicate an magnitude order. Thus, we observe that evaluated critical values with the simulation are significantly lower than the experimental values. The main reason of this difference is that residual elaboration stress that put the fiber in compression (binding) have not been taken in account. It is the next objective given to the continuation of this study.

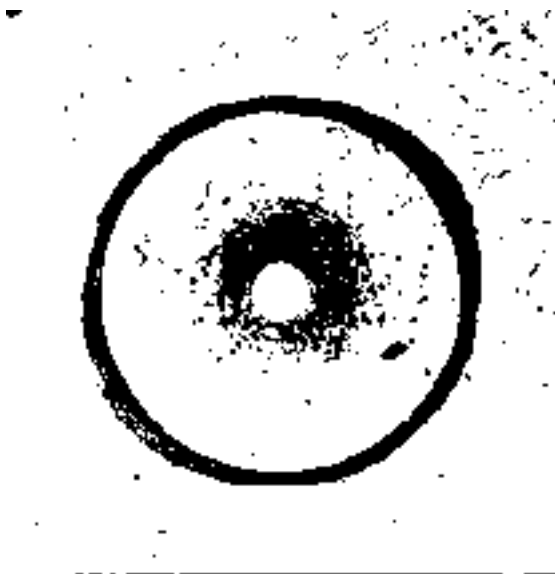


Fig 8 - Debonding micrography

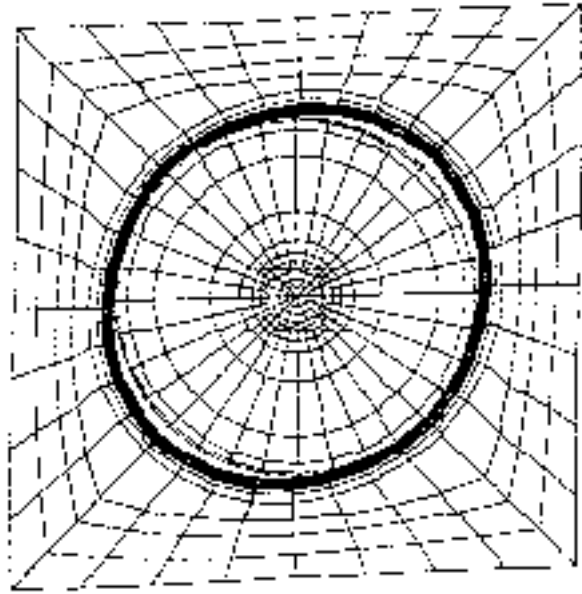


Fig. 9 - Debonding simulation

### Mesoscopic Debonding Criterion

If  $\epsilon$  is the mesoscopic strain tensor, we can write a debonding criterion at the scale of the homogeneous material as a quadratic form of its components :

$$\left( \frac{\epsilon_{11}}{\epsilon_{11}^c} \right)^2 + \left( \frac{\epsilon_{22}}{\epsilon_{22}^c} \right)^2 + \left( \frac{\epsilon_{33}}{\epsilon_{33}^c} \right)^2 + \left( \frac{\epsilon_{23}}{\epsilon_{23}^c} \right)^2 + \left( \frac{\epsilon_{13}}{\epsilon_{13}^c} \right)^2 + \left( \frac{\epsilon_{12}}{\epsilon_{12}^c} \right)^2 = 1$$

where  $\epsilon_{11}^c$ ,  $\epsilon_{22}^c$ ,  $\epsilon_{33}^c$ ,  $\epsilon_{23}^c$ ,  $\epsilon_{13}^c$  and  $\epsilon_{12}^c$  represent the different critical debonding values. It is the finite element resolution of the six localization problems of the homogenization that allow to determine these values in seeking for each of them from what mesoscopic deformation the debonding takes place. This is obtain using the finite element similar to a spring (penalty) placed to the place of the possibly debonding, and whose behaviour of typical whole-or-nothing is governed by the preceding microscopic criterion.

## Simulation of Transversal Tensile Tests

The goal now is to simulate a transversal tests at room temperature on a SiC-Ti specimen (without titanium layers) called S0 where the axis of the specimen are the same as the axis of SiC-Ti material defined in figure 3. The mesoscopic debonding criterion is known. We can thus obtain the value of the stress tensor from which the debonding starts. We found that the starting value of the debonding is very different between the experiment and the simulation (error : 200%). This is because the manufacturing residual stresses have not been considered. We will see in the next section wether the result for the transverse tensile test can be improved by considering the manufacturing residual stresses.

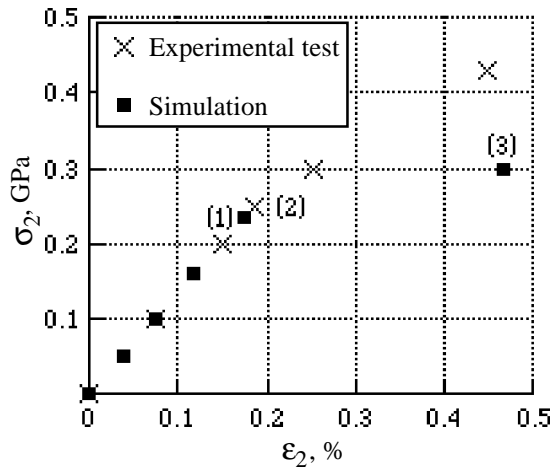
### ANALYSIS WITH CONSIDERATION OF THE RESIDUAL STRESSES

#### Manufacturing Residual Stresses

A quarter of the cell applying symmetric conditions on the axes and thus we obtain the manufacturing residual stresses [4].

#### Identification of a Microscopic and a Mesoscopic Debonding Criterion and Simulation of Transversal Tensile Tests

Using the same microscopic and mesoscopic criterion equations and proceeding as in the case without residual stresses, we determine first the characteristics of the local debonding criterion ( $\epsilon_{T^c}$ ,  $s_{N^c}$ ) and thus those of the mesoscopic one ( $\epsilon_{11^c}$ ,  $\epsilon_{22^c} = \epsilon_{33^c}$ ,  $\epsilon_{23^c}$ ,  $\epsilon_{13^c} = \epsilon_{12^c}$ ). Using the new identified critical values in the mesoscopic criterion, the simulated value agrees well with the experimental value (Fig. 10).



- (1) : simulated debonding start, (2) : experimental debonding start  
 (3) : simulated point giving the elastic slope of the completely damaged material

Fig. 10 - S0 specimen transverse tensile test at room temperature.  
 Simulation with consideration of the manufacturing residual stresses



## CONCLUSION

The debonding phenomenon between the fibre and the matrix was studied in a long fibre SiC-Ti metal-matrix composite. The debonding between the two constituents occurred by the rupture in the carbon interphase.

The analysis was both numerical and experimental and realized in a qualitative and quantitative ways. It shown the feasibility of the following methodology : to determine quantities at the scale of the homogeneous material from microscopic informations and observations (i.e. at the scale of the constituents of the material). An exemple is given for the determination of a mesoscopic debonding criterion. This work is realized without and with consideration of the manufacturing residual stresses. The conclusion is that they have a very significant role in the determination of the critical debonding values.

The use of numerical techniques for the experimental analysis seems increasingly necessary because of the complexity of the microstructures of the composite materials and the complexity of the phenomena involved. Although the calculation did not solved all problems, it has partly removed some ambiguities and has led to more finest understanding of the phenomena.

**ACKNOWLEDGEMENT** : The authors wish to thank the SNECMA (Société Nationale d'Etudes et de Construction de Moteurs d'Avions) for providing all the samples and the financial support. Authors want also thank Mr. Y. FAVRY and Mr. J.C. TEISSEBRE for their assistance with the realization of tests.

## REFERENCES

1. Renard J., "Modelling of a Damaged Composite Specimen by a Micro-Macro numerical Simulation", *Proceedings of the thirteen annual ASME-ETCE Composite Materials Symposium*, P. 57 - 62, 1990
2. Yang C.J., Jeng S.M. Yang J.M., "Interfacial Properties Measurement for SiC Fiber reinforced Titanium Alloy Composites", *Scripta Metallurgica and Materials*, 24, p. 469 - 474, 1990
3. Robertson J.G., "Manufacture and properties of Sigma-Fibre reinforced Titanium", *Agard Report n° 796*, (1994), pp. 71-78
4. Thionnet A., Renard J., "Micromechanical modelling of fibre/matrix interface effects in transversely loaded SiC/Ti-6-4 metal-matrix composites", *Composites Sciences and Technology*, **58**, (1998), pp. 945-955, 1998